We are IntechOpen, the world's leading publisher of Open Access books Built by scientists, for scientists

4,800
Open access books available

122,000
International authors and editors

135M
Downloads

Our authors are among the

154
Countries delivered to

TOP 1%
most cited scientists

12.2%
Contributors from top 500 universities

CLARIVATE ANALYTICS BOOK CITATION INDEX INDEXED

WEB OF SCIENCE™

Selection of our books indexed in the Book Citation Index in Web of Science™ Core Collection (BKCI)

Interested in publishing with us?
Contact book.department@intechopen.com

Numbers displayed above are based on latest data collected.
For more information visit www.intechopen.com

13

Intelligent Approach to MPPT Control Strategy for Variable-Speed Wind Turbine Generation System

Whei-Min Lin and Chih-Ming Hong
Department of Electrical Engineering,
National Sun Yat-Sen University
Kaohsiung 80424
Taiwan, R.O.C.

1. Introduction

Recently, wind generation systems are attracting great attentions as clean and safe renewable power sources. Wind generation can be operated by constant speed and variable speed operations using power electronic converters. Variable speed generation is attractive because of its characteristic to achieve maximum efficiency at all wind velocities (Pena et al. 2000; Senjyu et al. 2006; Sakamoto et al. 2006; Ramtharan et al. 2007; Fernandez et al. 2008), the improvement in energy production, and the reduction of the flicker problem. In the variable-speed generation system, the wind turbine can be operated at the maximum power operating point for various wind speeds by adjusting the shaft speed. These characteristics are advantages of variable-speed wind energy conversion systems (WECS). In order to achieve the maximum power control, some control schemes have been studied.

A variable speed wind power generation system (WPGS) needs a power electronic converter and inverter, to convert variable-frequency, variable-voltage power into constant-frequency constant-voltage, to regulate the output power of the WPGS. Traditionally a gearbox is used to couple a low speed wind turbine rotor with a high speed generator in a WPGS. Great efforts have been placed on the use of a low speed direct-drive generator to eliminate the gearbox. Many of the generators of research interest and for practical use in wind generation are induction machines with wound-rotor or cage-type rotor (Simoes et al. 1997; Li et al. 2005; Karrari et al. 2005; Wang & Chang 2004). Recently, the interest in PM synchronous generators is increasing. High-performance variable-speed generation including high efficiency and high controllability is expected by using a permanent magnet synchronous (PMSG) for a wind generation system.

Previous research has focused on three types of maximum wind power extraction methods, namely tip speed ratio (TSR) control, power signal feedback (PSF) control and hill-climb searching (HCS) control. TSR control regulates the wind turbine rotor speed to maintain an optimal TSR. PSF control requires the knowledge of the wind turbine's maximum power curve, and tracks this curve through its control mechanisms. Among previously developed wind turbine maximum power point tracking (MPPT) strategies, the TSR direction control method is limited by the difficulty in wind speed and turbine speed measurements

(Thiringer & Linders 1993; Chedid et al. 1999; Tanaka & Toumiya 1997; Morimoto et al. 2005; Koutroulis & Kalaitzakis 2006). Many MPPT strategies were then proposed to eliminate the measurements by making use of the wind turbine maximum power curve, but the knowledge of the turbine's characteristics is required. HCS control has been proposed to continuously search for the peak output power of the wind turbine. In comparison, the HCS MPPT is popular due to its simplicity and independence of system characteristics. In this paper, a Wilcoxon radial basis function network (WRBFN)-based with HCS MPPT strategy is proposed for PMSG wind turbine generator (WTG). The proposed control structure, WRBFN with modified particle swarm optimization (MPSO) algorithm is forces the system to reach its equilibriums quickly where the turbine inertia effect is minimized. HCS can be fast and effective in spite of the variations in wind speeds and the presence of turbine inertia.

Intelligent control approaches such as neural network and fuzzy system do not require mathematical models and have the ability to approximate nonlinear systems. Therefore, there were many researchers using intelligent control approaches to represent complex plants and construct advanced controllers. Moreover, the locally tuned and overlapped receptive field is a well-known structure that has been studied in regions of cerebral cortex, visual cortex, and so on (Jang & Sun 1997). Based on the biological receptive fields, the RBFN that employs local receptive fields to perform function mappings was proposed in (Jang & Sun 1993). Furthermore, the RBFN has a similar feature to the fuzzy system. First, the output value is calculated using the weighted sum method. Second, the number of nodes in the hidden layer of the RBFN is the same as the number of if-then rules in the fuzzy system. Finally, the receptive field functions of the RBFN are similar to the membership functions of the premise part in the fuzzy system. Therefore, the RBFN is very useful to be applied to control the dynamic systems (Seshagiri & Khail 2000).

2. Analysis of wind generation system

2.1 Wind turbine characteristics and modeling

In order to capture the maximal wind energy, it is necessary to install the power electronic devices between the WTG and the grid where the frequency is constant. The input of a wind turbine is the wind and the output is the mechanical power turning the generator rotor (Li et al. 2005; Karrari et al. 2005; Wang & Chang 2004). For a variable speed wind turbine, the output mechanical power available from a wind turbine could be expressed as

$$P_m = \frac{1}{2}\rho A C_p(\lambda,\beta)V_\omega^3 \tag{1}$$

where ρ and A are air density and the area swept by blades, respectively. V_ω is the wind velocity (m/s), and C_p is called the power coefficient, and is given as a nonlinear function of the tip speed ratio (TSR) λ defined by

$$\lambda = \frac{\omega_r r}{V_\omega} \tag{2}$$

where r is wind turbine blade tip radius, and ω_r is the turbine speed. C_p is the function of the λ and the blade pitch angle β, general defined as follows:

$$C_p = 0.73(\frac{151}{\lambda_i} - 0.58\beta - 0.002\beta^{2.14} - 13.2)e^{\frac{-18.4}{\lambda_i}}$$
$$\lambda_i = \frac{1}{\frac{1}{\lambda - 0.02\beta} - \frac{0.003}{\beta^3 + 1}} \quad (3)$$

By using (3), the typical C_P versus λ curve is shown in Fig. 1. In a wind turbine, there is an optimum value of TSR λ_{opt} that leads to maximum power coefficient $C_{p\max}$. When TSR in (2) is adjusted to its optimum value $\lambda_{opt} = 6.9$ with the power coefficient reaching $C_{p\max} = 0.4412$, the control objective of the maximum power extraction is achieved.

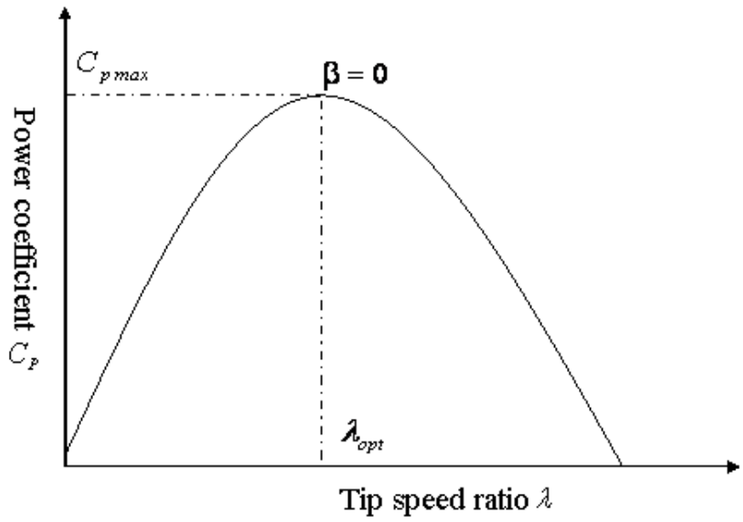

Fig. 1. Typical C_P versus λ curve

2.2 PMSG

The wind generator is a three-phase PMSG, where the mechanical torque (T_m) and electrical torque (T_e) can be expressed as

$$T_m = \frac{P_m}{\omega_r} \quad (4)$$

$$T_e = \frac{P_e}{\omega_e} = \frac{2}{P}\frac{P_e}{\omega_r} \quad (5)$$

In general, the mechanical dynamic equation of a PMSG is given by

$$J\frac{d\omega_r}{dt} = T_m - (P/2)T_e \quad (6)$$

where ω_e and P are electrical angular frequency, and the number of poles. J is the inertia moment of WTG.

2.3 Wind turbine emulation

The emulation of the wind turbine is implemented by a dc motor drive with torque control. In the prototype, a 1.5kW, 1980rpm dc motor was used. A computer program reads the wind input file obtained with various test conditions, and calculates the wind turbine torque by taking into account wind velocity, turbine rotational speed, and the wind turbine power coefficient curve. The control algorithms for turbine emulation are implemented in a control board dSPACE DS1102. This board is a commercial system designed for rapid prototyping of real control algorithms; it is based on the Texas Instruments TMS320C32 floating-point DSP. The DS1102 board is hosted by a personal computer.

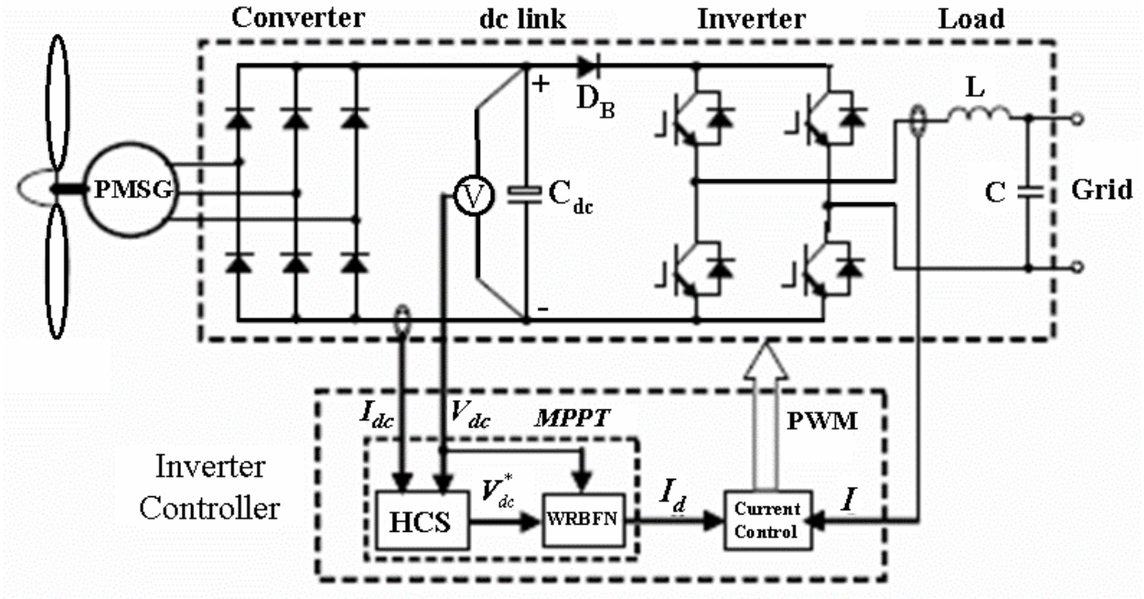

Fig. 2. PMSG WT generation system

3. HCS control method

3.1 System configuration

Fig. 2 presents the block diagram of the WT generation system in our research, where a PMSG is driven by a WT to feed the extracted power from wind resources to the grid through a single-phase inverter. A variable speed WPGS needs a power electronic converter and inverter, to convert variable-frequency, variable-voltage AC power from a generator to DC and then into constant-frequency constant-voltage power. In the dc-link of the inverter, a blocking diode D_B is used to improve the power delivering capability as well as to guarantee that the dc-link voltage transfers to the output voltage. An inverter controller is designed to deal with two aspects, the MPPT control for power maximization and the the current control for output PWM to inverter. The dc-link voltage and current, V_{dc} and I_{dc} are sampled to provide the power ($P_{dc} = V_{dc} \cdot I_{dc}$) input to the controller, and V_{dc} reference signal V_{dc}^* is updated in real time using an HCS method so as to lead the system to its optimal operation point. On the other hand, a WRBFN controller is designed to force V_{dc} to follow V_{dc}^* by adjusting the load current reference for the inverter current controller.

3.2 Optimal DC-link voltage (V_{dc}) search

From the C_P - λ characteristics, the turbine mechanical power P_m can be shown as a function of V_{dc}, and an optimal V_{dc} exists for the maximum P_m output, provided that a PMSG is employed in the generation system. Fig. 3 shows a group of P_m - V_{dc} curves and the corresponding maximum power curve formed with various optimal operating points, where wind speeds $u1 < u2 < u3 < u4$. In order to extract maximum power from wind, the optimal V_{dc} is searched in real time using the HCS method. With HCS, if the previous increment of V_{dc}^* is followed by an increase of P_m, then the search of V_{dc}^* continues in the same direction; otherwise, the search reverses its direction. An example can be seen in Fig. 3, where the wind change from $u3 \to u4 \to u2$ with the search of V_{dc} from $A \to B \to C \to D \to E$. The increment of P_m is approximated by that of P_{dc} , and the search is executed at dynamic equilibrium operation points where P_{dc} is approximately equal to P_m and the effect of turbine inertia J can be minimized. In dynamic states, V_{dc}^* will be held and the WRBFN will adjust the load current in real time to drive the system to its equilibrium point as soon as possible. Fig. 3 illustrates the searching process $(ABCDE)$ for the maximum power points when the wind speed varies.

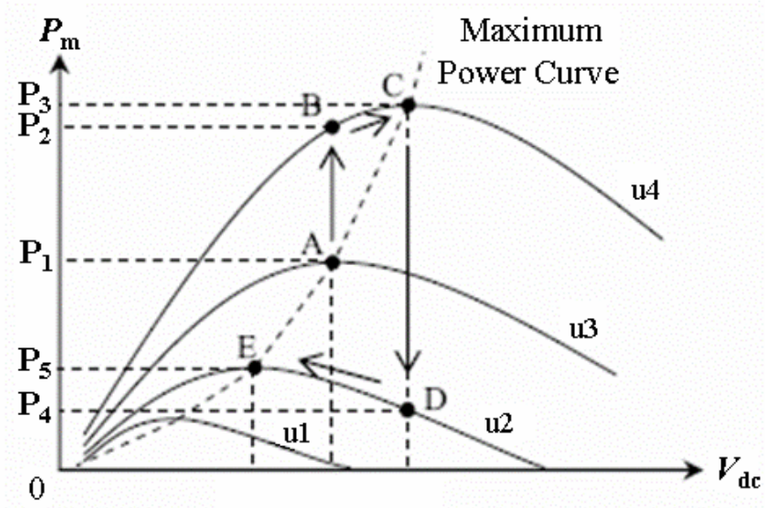

Fig. 3. Principle of HCS control method.

4. The proposed intelligent MPPT control algorithm

4.1 Wilcoxon radial basis function network

The linear Wilcoxon regressor is quite robust against outliers (Hogg et al. 2005), which motivates the design of wilcoxon neural networks. A three-layer neural network shown in Fig. 4 is adopted to implement the proposed WRBFN. The WRBFN with MPSO controller is used, and the control law I_d is generated from the WRBFN The WRBFN input is $x_1^{(1)}$ and $x_2^{(1)}$ of the first layer, where $x_1^{(1)} = V_{dc} - V_{dc}^* = e$ and $x_2^{(1)} = \dot{e}$ in this study. In the proposed WRBFN, the units in the input, hidden, and output layers are two, nine and one, respectively. The signal propagation and the basic function in each layer can be found (Lin & George Lee 1996).

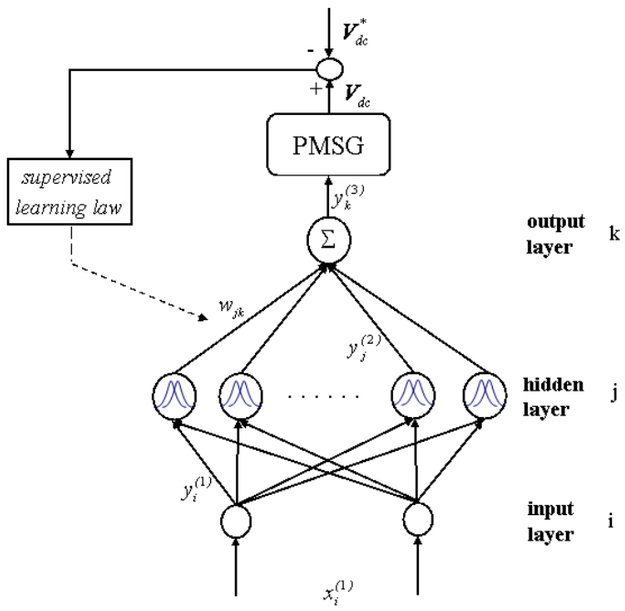

Fig. 4. Architecture of the WRBFN

Layer 1 : input layer

The nodes at this layer are used to directly transmit the numerical inputs to the next layer. That is, for the *i*th node of layer 1, the net input and output are defined by

$$\begin{aligned} net_i^{(1)} &= x_i^{(1)}(N) \\ y_i^{(1)}(N) &= f_i^{(1)}\left(net_i^{(1)}(N)\right) = net_i^{(1)}(N) \qquad i = 1,2 \end{aligned} \tag{7}$$

Layer 2 : hidden layer

At this layer, every node performs a Gaussian basis function. The Gaussian basis function, a particular example of radial basic functions, is used here as a membership function. Then

$$\begin{aligned} net_j^{(2)}(N) &= -\sum_{i=1}^{n}(x_i^{(1)} - c_{ij})^2 / v_{ij} \\ y_j^{(2)}(N) &= f_j^{(2)}\left(net_j^{(2)}(N)\right) = \exp\left(net_j^{(2)}(N)\right) \qquad j = 1,...,9 \end{aligned} \tag{8}$$

where $c_j = \begin{bmatrix} c_{1j} & c_{2j} & \cdots & c_{ij} \end{bmatrix}^T$ and v_{ij} denote respectively, the mean and the standard deviation (STD) of the Gaussian basis function.

Layer 3 : output layer

The single node k in this layer is denoted by Σ, which computes the overall output as the summation of all incoming signals by

$$\begin{aligned} net_k^{(3)} &= \sum_{j-1}^{m} w_{jk} y_j^{(2)}(N), \\ y_k^{(3)}(N) &= f_k^{(3)}(net_k^{(3)}(N)) = net_k^{(3)}(N) = I_d \end{aligned} \tag{9}$$

where the connection weight w_{jk} is the connective weight between the hidden node, and the output layer k.

4.2 The network training and learning process

Once the WRBFN has been initialized, a supervised learning law is used to train this system. The basis of this algorithm is gradient descent. The derivation is the same as that of the back-propagation algorithm. It is employed to adjust the parameters w_{jk}, c_{ij}, v_{ij} of the WRBFN by using the training patterns. By recursive application of the chain rule, the error term for each layer is first calculated. The adaptation of weights to the corresponding layer is then given. The purpose of supervised learning is to minimize the error function *E* expressed as

$$E = \frac{1}{2}\left(V_{dc} - V_{dc}^{*}\right)^2 = \frac{1}{2}e_L^2 \tag{10}$$

where V_{dc}^{*} and V_{dc} represent the dc-link voltage reference and actual dc-link voltage feedback of the generator.

Layer 3 : update weight w_{jk}

At this layer, the error term to be propagated is given by

$$\delta_k = -\frac{\partial E}{\partial net_k^{(3)}} = \left[-\frac{\partial E}{\partial y_k^{(3)}}\frac{\partial y_k^{(3)}}{\partial net_k^{(4)}}\right] \tag{11}$$

Then the weight w_{jk} is adjusted by the amount

$$\Delta w_{jk} = -\frac{\partial E}{\partial w_{jk}} = \left[-\frac{\partial E}{\partial y_k^{(3)}}\frac{\partial y_k^{(3)}}{\partial net_k^{(3)}}\right]\left(\frac{\partial net_k^{(3)}}{\partial w_{jk}}\right) = \delta_k y_j^{(2)} \tag{12}$$

We have

$$w_{jk}(N+1) = w_{jk}(N) + \eta_w \Delta w_{jk}(N) \tag{13}$$

where η_w is the learning rate for adjusting the parameter w_{jk}.

Layer 2 : update c_{ij} and v_{ij}

The multiplication operation is done in this layer. The adaptive rule for c_{ij} is

$$\Delta c_{ij} = -\frac{\partial E}{\partial c_{ij}} = \left[-\frac{\partial E}{\partial net_k^{(3)}}\frac{\partial net_k^{(3)}}{\partial y_j^{(2)}}\frac{\partial y_j^{(2)}}{\partial c_{ij}}\right] = \delta_k w_{jk} y_j^{(2)}\frac{2\left(x_i^{(1)} - c_{ij}\right)}{v_{ij}} \tag{14}$$

and the adaptive rule for v_{ij} is

$$\Delta v_{ij} = -\frac{\partial E}{\partial v_{ij}} = \left[-\frac{\partial E}{\partial net_k^{(3)}}\frac{\partial net_k^{(3)}}{\partial y_j^{(2)}}\frac{\partial y_j^{(2)}}{\partial v_{ij}}\right] = \delta_k w_{jk}\frac{2\left(x_i^{(1)} - c_{ij}\right)^2}{\left(v_{ij}\right)^2} \tag{15}$$

We have

$$\begin{aligned} c_{ij}(k+1) &= c_{ij}(k) + \eta_m \Delta c_{ij} \\ v_{ij}(k+1) &= v_{ij}(k) + \eta_\sigma \Delta v_{ij} \end{aligned} \tag{16}$$

where η_m and η_σ are the learning rates for adjusting the parameters c_{ij} and v_{ij}, respectively. The exact calculation of the jacobian of the system, which is contained in $\partial E / \partial y_k^{(3)}$, cannot be determined due to the uncertainty of the PMSG dynamic. To overcome this problem and to increase the on-line learning ability of the connective weights, the delta adaptation law (Lin & George Lee 1996) is implemented as follows to solve the difficulty

$$\delta_k \equiv e_L + \dot{e}_L$$

The learning rates η_w, η_m, η_σ are adjusted by MPSO as stated below.

5. WRBFN learning rates adjustment using MPSO

PSO is a population-based optimization method first proposed by Kennedy and Eberhart. PSO technique finds the optimal solution using a population of particles. Each particle represents a candidate solution to the problem. PSO is basically developed through simulation of bird flocking in two-dimensional space (Esmin et al. 2005).

Step 1: Define basic conditions

In the first step of MPSO, one should determine the parameters that need to be optimized and give them minimum and maximum ranges. The number of groups, population size of each group, and initial radius of each *gbest* are also assumed in this step.

Step 2: Initialize random swarm location and velocity

To begin, initial location $R_i^d(N)$ and velocities $v_i^d(N)$ of all particles are generated randomly in whole search space. Moreover, the population size is set to $P = 15$ and the dimension of the particle is set to $d = 3$ in this study. The generation particles are $R_i^d = [R_i^1, R_i^2, R_i^3]$, where R_i^1, R_i^2, R_i^3 are the RBFN learning rates, respectively. The initial *pbest* of a particle is set by its current position. Then, *gbest* of a group is selected among the *pbests* in the group.
The random generation of $R_i^d(N)$ initial value ranged as

$$R_i^d \sim U[\eta_{\min}^d, \eta_{\max}^d]$$

where $\eta_{\min}, \eta_{\max}$ are the lower and upper bound of the learning rates.

Step 3:Update velocity

In the classical PSO algorithm, the velocity of a particle was determined according to the relative location from *pbest* and *gbest.*
During each iteration, every particle in the swarm is updated using (17) and (18). Two pseudorandom sequences $r_1 \sim U(0,1)$ and $r_2 \sim U(0,1)$ are used to produce the stochastic nature of the algorithm. For dimensions *d*, let R_i^d, $Pbest_i^d$, and v_i^d be the current position, current personal best position. The velocity update step is

$$v_i^d(N+1) = wv_i^d(N) + c_1 \cdot r_1 \cdot (Pbest_i^d - R_i^d(N)) + c_2 \cdot r_2 \cdot (Gbest^d - R_i^d(N)) \quad (17)$$

Step 4: Update position

The new velocity is then added to the current position of the particle to obtain its next position

$$R_i^d(N+1) = R_i^d(N) + v_i^d(N+1) \quad i = 1,\ldots,P \quad (18)$$

Step 5: Update *pbests*

If the current position of a particle is located within the analysis space and does not intrude territory of other *gbests*, the objective function of the particle is evaluated. If the current fitness is better than the old *pbest* value, *pbest* is replaced by the current position. The fitness value of each particle is calculated by

$$FIT = \frac{1}{0.1 + abs(V_{dc} - V_{dc}^*)} \quad (19)$$

Step 6: Update *gbests*

In the conventional PSO, *gbest* is replaced by the best *pbest* among the particles. However, when such a strategy is applied to multimodal function optimization, some *gbests* of different groups can be overlapped. To maintain fast convergence rate of PSO, *gbest* of the group could be selected among the $Pbest_i^d = [Pbest_1^d, Pbest_2^d, \ldots Pbest_p^d]$ having high fitness value.

Step 7: Repeat and check convergence

Steps 3-6 are repeated until all particles are gathered around the *gbest* of each group, or a maximum iteration number is encountered. The final $Gbest_i^d$ is the optimal learning rate $(\eta_w, \eta_m, \eta_\sigma)$ of RBFN.

The inertia weight w in (17) is used to control the convergence behavior of the PSO. Small w results in rapid convergence usually on a suboptimal position, while a large value may cause divergence. In this paper, the inertia weight w is set according to the equation that

$$w = w_{\max} - \frac{w_{\max} - w_{\min}}{iter_{\max}} \cdot iter \quad (20)$$

where $iter_{\max}$ is maximum number of iterations, and *iter* is the current iteration number.

6. Experimental results

The WRBFN with MPSO performance is compared with two baseline controllers: the fuzzy (Chen et al. 2000) and the proportional-integral (PI) controller. The WRBFN with MPSO, fuzzy and PI methods were tested through experimental. The obtained performance with the different controllers are shown in Fig. 5 to Fig. 7, and summarized in Table 1. Various

cases were conducted, the wind profile is simulation with a 5*msec* sampling time the wind profile is assumed a volatile sinusoidal wave. The conventional PI type controller is widely used in the industry due to its simple control structure, ease of design and inexpensive cost. The average power of PI is compared with that of WRBFN with MPSO algorithm and Fuzzy-Based algorithm.

The WTG system used for the experimental has the following parameters:

1. Wind turbine parameters:

$$P_m = 750W\ ;\ 3.75A\ \ ;\ 3000r/\min\ ;\ \rho = 1.25kg/m^3\ ;\ r = 0.5m\ ;\ J = 1.32\times10^{-3}Nm\sec^2$$

2. Generator parameters:

$$R\ = 1.47\Omega\ ; L_d = L_q = 5.33mH\ ;\ L_{md} = 4.8mH\ ;\ I_{fd} = 46.75A\ ;\ K_t = 0.6732Nm/A$$

6.1 PI algorithm for V_{dc} control

The WRBFN with MPSO algorithm replaced by PI algorithm is shown in Fig. 2. Fig. 5 illustrates the experimental result for PI control. The average power is 205W for the same period. It can be found that TSR is always round 6.9 and C_p is 0.4412. The verification of maximum power tracking control is shown in Fig. 5(a). The dc-link voltage tracking response is shown in Fig. 5(b). Fig. 5(c) and 5(d) shows power coefficient C_p and TSR λ.

6.2 Fuzzy-based algorithm for V_{dc} control

The WRBFN with MPSO algorithm replace by Fuzzy-Based algorithm as shown in Fig. 2. A fuzzy logic control (FLC) algorithm is characterized by "IF-THEN" rules. The algorithm is suitable for wind turbine control with complex nonlinear models and parameters variation. The input variables of Fuzzy-Based MPPT are dc-link power tracking error and the difference of dc-link power tracking error.

Fig. 6 shows that 217W (an increase of 5.36% compared with that of PI control) is obtained by the Fuzzy-Based algorithm during the 50 sec. It can be found that λ and C_p are close to the optimal values of 6.9 and 0.4412, respectively. The wind speed profiles of turbine power P_m and dc-link power P_{dc} are also shown in Fig. 6(a). The dc-link voltage tracking response is shown in Fig. 6(b). Fig. 6(c) and 6(d) are shows that power coefficient C_p and TSR λ.

6.3 WRBFN with MPSO algorithm for V_{dc} Control

WRBFN with MPSO algorithm control is considered and the experimental result is shown in Fig. 7. The verification of maximum power tracking control is shown in Fig. 7(a), where the wind speed profiles of turbine power P_m and dc-link power P_{dc} are also shown. The dc-link voltage tracking response is shown in Fig. 7(b). Fig. 7(c) shows power coefficient C_p which is close to its maximum value during the whole wind speed profile, same for λ of Fig. 7(d). The efficiency of the maximum power extraction can be clearly observed as the power coefficient is fixed at the optimum value $C_p = 0.4412$ and $\lambda = 6.9$. The average power is 224W. Compared with that from the PI control method, it increases by 9.27%.

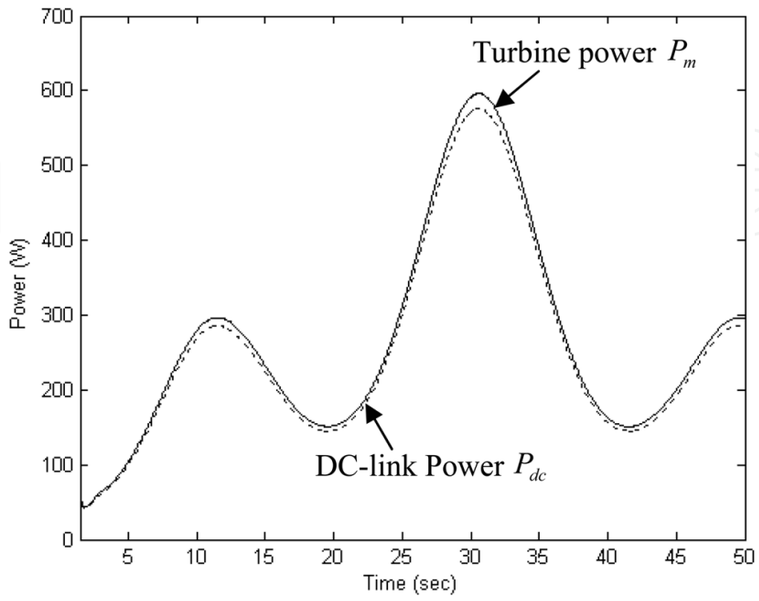
Turbine power P_m
DC-link Power P_{dc}
Power (W)
Time (sec)
0
100
200
300
400
500
600
700
5
10
15
20
25
30
35
40
45
50

(a)

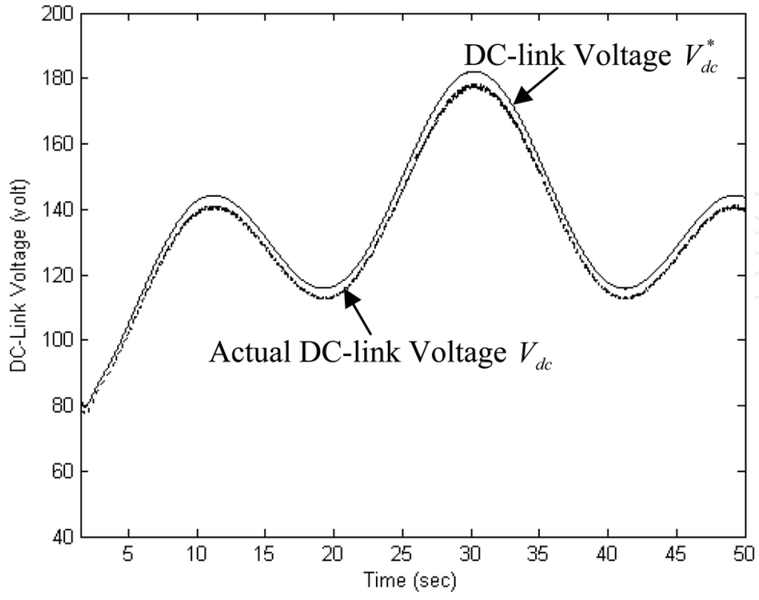
DC-link Voltage V_{dc}^*
Actual DC-link Voltage V_{dc}
DC-Link Voltage (volt)
Time (sec)
40
60
80
100
120
140
160
180
200
5
10
15
20
25
30
35
40
45
50

(b)

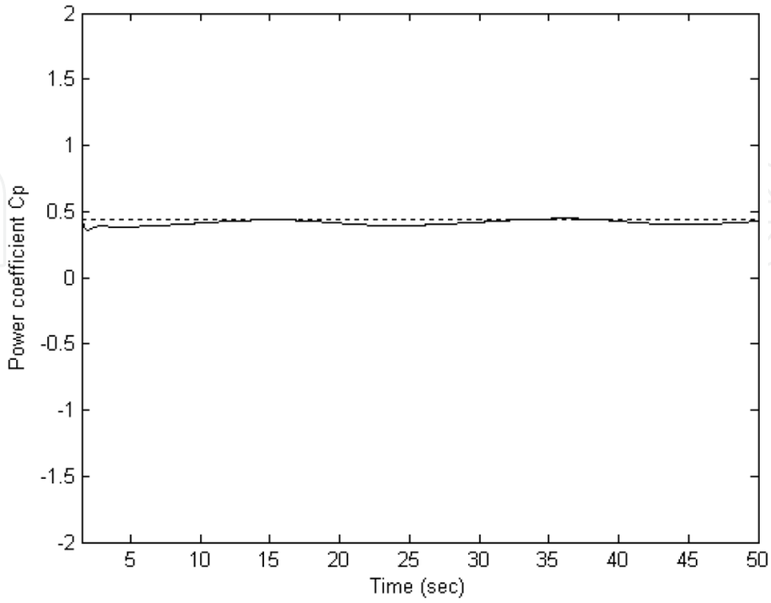

(c)

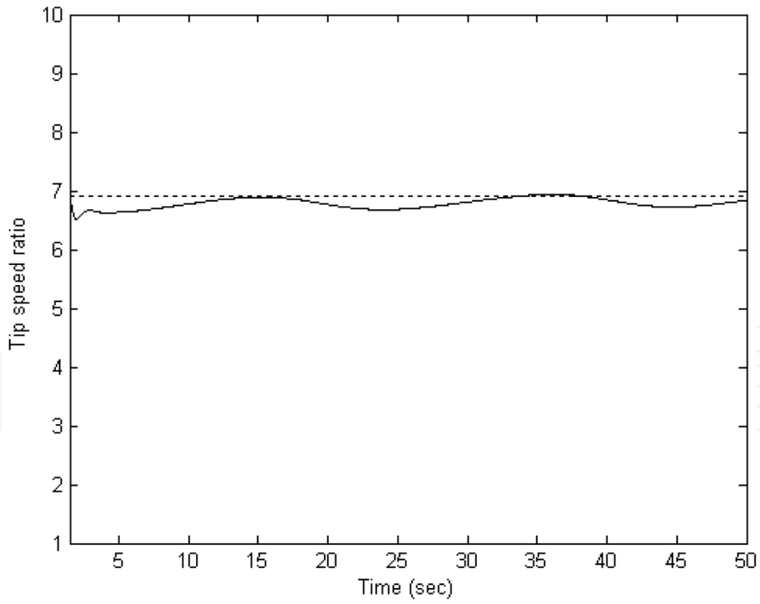

(d)

Fig. 5. Experimental results of the wind speed profile : (a)The maximum power tracking control signal. (b)The dc-link voltage tracking response. (c)Power coefficient $C_{p.}$ (d)Tip-speed ratio λ .

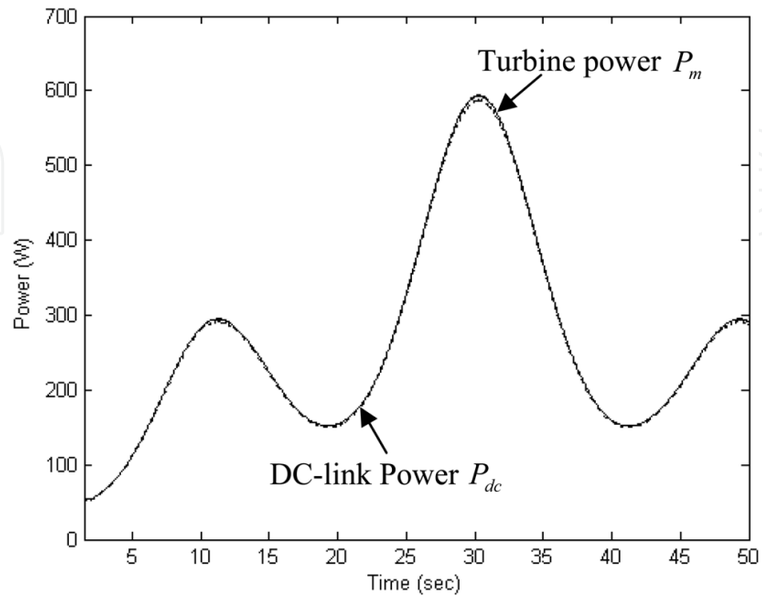
Turbine power P_m
DC-link Power P_{dc}
Power (W)
Time (sec)
0
100
200
300
400
500
600
700
5
10
15
20
25
30
35
40
45
50

(a)

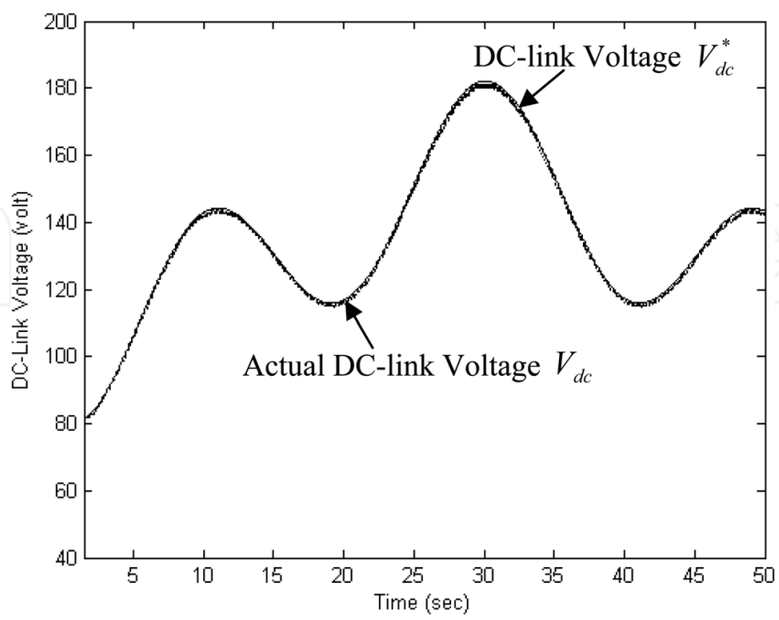
DC-link Voltage V_{dc}^*
Actual DC-link Voltage V_{dc}
DC-Link Voltage (volt)
Time (sec)
40
60
80
100
120
140
160
180
200
5
10
15
20
25
30
35
40
45
50

(b)

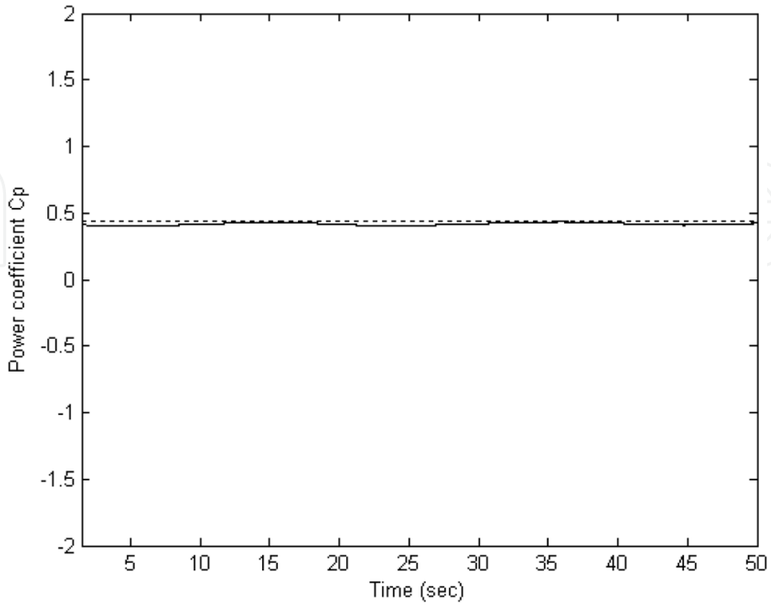

(c)

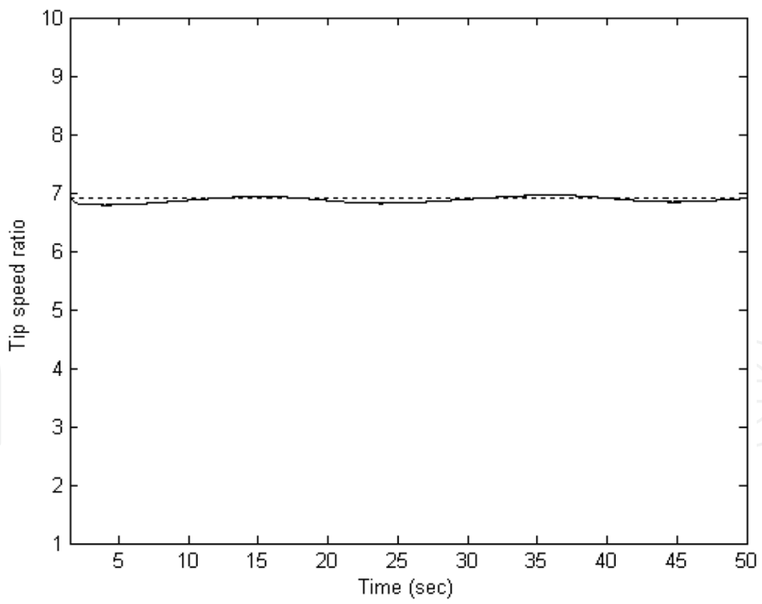

(d)

Fig. 6. Experimental results of the wind speed profile : (a)The maximum power tracking control signal. (b)The dc-link voltage tracking response. (c)Power coefficient $C_{p.}$ (d)Tip-speed ratio λ .

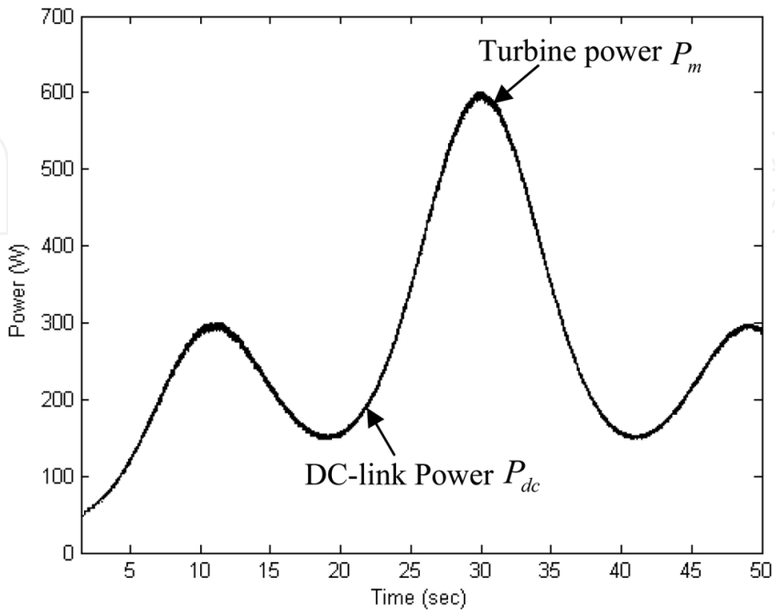
Turbine power P_m
DC-link Power P_{dc}
Power (W)
Time (sec)
0
100
200
300
400
500
600
700
5
10
15
20
25
30
35
40
45
50

(a)

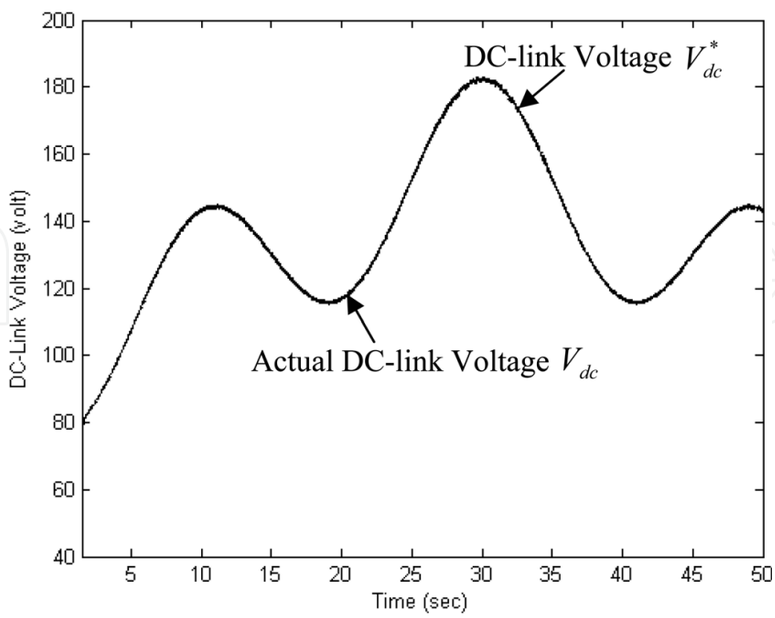
DC-link Voltage V_{dc}^*
Actual DC-link Voltage V_{dc}
DC-Link Voltage (volt)
Time (sec)
40
60
80
100
120
140
160
180
200
5
10
15
20
25
30
35
40
45
50

(b)

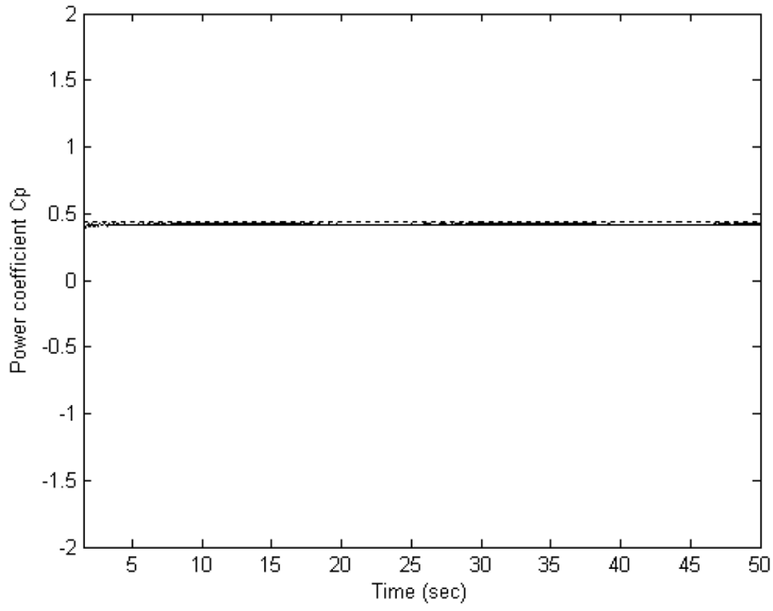

(c)

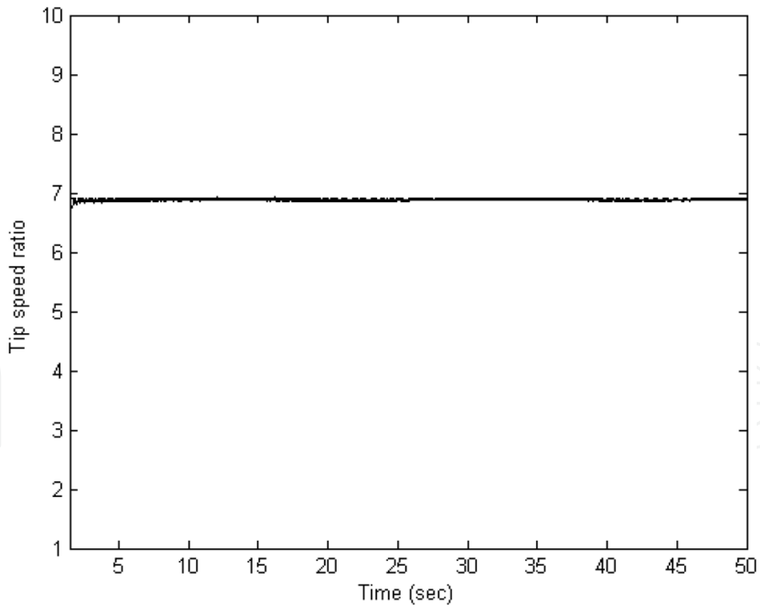

(d)

Fig. 7. Experimental results of the wind speed profile : (a)The maximum power tracking control signal. (b)The dc-link voltage tracking response. (c)Power coefficient $C_{p.}$ (d)Tip-speed ratio λ .

Control Characteristic / Controller Type	Average Power (P_{dc}) (W)	Increasing power percentage (%)	Max. error of power coefficient (C_p) (%)	Max. error of DC-link power (%)	Max. error of DC-link voltage (%)
WRBFN with MPSO algorithm method	224	9.27	1.79	0.32	0.074
Fuzzy-Based algorithm method	216	5.36	9.95	1.4	0.9
PI method	205	----	18.4	2.58	2.25

Table 1. Performance for various control methods

From the performance comparison for various methods above experimental results, we can see that MPPT is important for either high or low wind speeds, as shown in Table 1. Table 1 shows the average power, maximum error of power coefficient, maximum error of dc-link power and percentage of power increase from each control method. On the other hand, the maximum error of the power coefficient is around 23% in [9], and the maximum power deviation is about 7% in [14]. The proposed method in comparison with other methods [9,14] has better performance.

7. Conclusion

This paper focuses on the development of maximum wind power extraction algorithms for inverter-based variable speed WPGS. The HCS method is proposed in this paper for maximum power searching with various turbine inertia. Without a need for measurements of wind speed and turbine rotor speed, HCS is simple to implement. When exciting the system with a real wind profile, the system is able to track maximum power using generated power as input. The proposed system has been implemented, with a commercial PMSG and a dc drive to emulate the wind turbine behavior. The process is running in a dSPACE board that includes a TMS320C32 floating-point DSP. Experimental results show the appropriate behavior of the system.

Three MPPT control algorithms are proposed in this paper, without any wind speed sensor. It is found that the PI method can operate near the optimal *Cp*. However, the PI-type controller may not provide perfect control performance if the controlled plant is highly nonlinear or the desired trajectory is varied with higher frequency. The proposed output maximization control of WRBFN can maintain the system stability and reach the desired performance even with parameter uncertainties.

8. References

Pena, R. S., Cardenas, R. J. , Asher G. M. & Clare J. C. (2000). Vector controlled indction machines for stand-alone wind energy applications, IEEE Industry Application Annu. Meeting, Vol.3, pp.1409-1415.

Senjyu, T., Sakamoto, R., Urasaki, N., Funabashi, T. & Sekine, H. (2006). Output Power Leveling of Wind Farm Using Pitch Angle Control with Fuzzy Neural Network. IEEE Power Engineering Society General Meeting, page(s):8pp.

Sakamoto, R., Senjyu, T., Sakamoto, R., Kaneko, T., Urasaki, N., Takagi, T., Sugimoto, S. & Sekine, H. (2006). Output Power Leveling of Wind Turbine Generator by Pitch Angle Control Using H_∞ Control, The IEEE PSCE Conf., pp. 2044-2049.

Ramtharan, G., Ekanayake, J. B. & Jenkins, N. (2007). Frequency support from doubly fed induction generator wind turbines, IET Renewable Power Generation, Vol. 1, No. 1, pp. 3-9.

Fernandez, L. M., Garcia, C. A. & Jurado, F. (2008). Comparative study on the performance of control systems for doubly fed induction generator (DFIG) wind turbines operating with power regulation, Energy, Vol. 33, Issue. 9, pp. 1438-1452.

Simoes, M. G., Bose, B. K. & Spiegel, R. J. (1997). Fuzzy logic-based intelligent control of a variable speed cage machine wind generation system, IEEE Transactions on Power Electronics, Vol. 12, No. 1, pp. 87-95.

Li, H., Shi, K. L. & McLaren, P. G. (2005). Neural-Network-Based Sensorless Maximum Wind Energy Capture with Compensated Power Coefficient, IEEE Transactions Industry Application, Vol. 41, No. 6, pp. 548-1556.

Karrari, M., Rosehart, W. & Malik, O. P. (2005). Comprehensive Control Strategy for a variable Speed Cage Machine Wind Generation Unit, IEEE Transactions on Energy Conversion, Vol. 20, No. 2, pp. 415-423.

Wang, Q. & Chang, L. (2004). An intelligent maximum power extraction algorithm for inverter-based variable speed wind turbine systems, IEEE Transactions Power Electronics, Vol. 19, No. 5, pp. 1242-1249.

Thiringer, T. & Linders J. (1993). Control by variable rotor speed of a fixed-pitch wind turbine operating in a wide speed range, IEEE Transactions Energy Conversion, Vol. EC-8, pp. 520-526.

Chedid, R., Mrad, F. & Basma, M. (1999). Intelligent control of a class of wind energy conversion systems, IEEE Transactions on Energy Conversion, Vol. EC-14, pp. 1597-1604.

Tanaka, T. & Toumiya, T. (1997). Output control by Hill-Climbing method for a small wind power generating system, Renewable Energy, Vol. 12, Issue. 4, pp. 387-400.

Morimoto, S., Nakamura, T., Sanada, M. & Takeda, Y. (2005). Sensorless Output Maximization Control for Variable-Speed Wind Generation System Using IPMSG, IEEE Transactions on Industry Applications, Vol.41, No.1, pp. 60-67.

Koutroulis, E. & Kalaitzakis, K. (2006). Design of a Maximum Power Tracking System for Wind-Energy-Conversion Applications, IEEE Transactions on Industrial Electronics, Vol. 53, No. 2, pp. 486-494.

Jang, J. S. R. & Sun, C. T. (1997). Neuro-Fuzzy and Soft Computing: A computational approach to learning and machine intelligenc. Upper Saddle River, NJ: Prentice-Hall.

Jang, J. S. R. & Sun, C. T. (1993). Function equivalence between radial basis function networks and fuzzy inference systems, IEEE Transactions on Neural Networks, Vol. 4, No. 1, pp. 156-159.

Seshagiri, S. & Khail, H. K. (2000). Output feedback control of nonlinear systems using RBF Function equivalence between radial basis function neural networks, IEEE Transactions Neural Networks, Vol. 11, No. 1, pp. 69-79.

Hogg, R. V., McKean, J. W. & Craig, A. T. (2005). Introduction to Mathematical Statistics. Sixth Edition, New Jersey: Prentice-Hall.

Lin, C. T. & George Lee, C. S. (1996). Neural Fuzzy Systems. Upper Saddle River, NJ:Prentice-Hall, Inc..

Esmin, A. A., Torres, G. L. & Souza, C. Z. (2005). A Hybrid Particle Swarm Optimization Applied to Loss Power Minimization, IEEE Transaction on Power Systems, Vol. 20, No. 2, pp. 859-866.

Chen, Z., Gomez, S. A. & McCormick, M. (2000). A fuzzy logic controlled power electronic system for variable speed wind energy conversion systems, Eighth International Conference on Power Electronics and Variable Speed Drives, pp. 114-119.

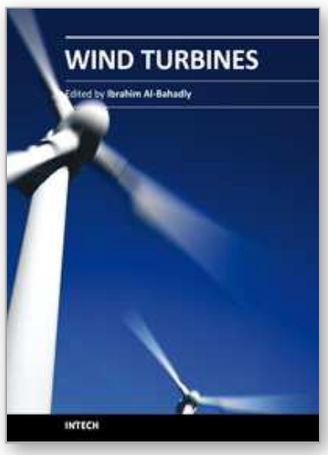

Wind Turbines

Edited by Dr. Ibrahim Al-Bahadly

ISBN 978-953-307-221-0
Hard cover, 652 pages
Publisher InTech
Published online 04, April, 2011
Published in print edition April, 2011

The area of wind energy is a rapidly evolving field and an intensive research and development has taken place in the last few years. Therefore, this book aims to provide an up-to-date comprehensive overview of the current status in the field to the research community. The research works presented in this book are divided into three main groups. The first group deals with the different types and design of the wind mills aiming for efficient, reliable and cost effective solutions. The second group deals with works tackling the use of different types of generators for wind energy. The third group is focusing on improvement in the area of control. Each chapter of the book offers detailed information on the related area of its research with the main objectives of the works carried out as well as providing a comprehensive list of references which should provide a rich platform of research to the field.

INTECH
open science | open minds

InTech Europe
University Campus STeP Ri
Slavka Krautzeka 83/A
51000 Rijeka, Croatia
Phone: +385 (51) 770 447
Fax: +385 (51) 686 166
www.intechopen.com

InTech China
Unit 405, Office Block, Hotel Equatorial Shanghai
No.65, Yan An Road (West), Shanghai, 200040, China
中国上海市延安西路65号上海国际贵都大饭店办公楼405单元
Phone: +86-21-62489820
Fax: +86-21-62489821

IntechOpen